High-temperature heat capacity and thermodynamic properties for end-member titanite (CaTiSiO5)

Article *in* Physics and Chemistry of Minerals · April 2001

DOI: 10.1007/s002690000124 · Source: OAI

2 authors, including:

Dimitris Xirouchakis
RSK Group plc
39 PUBLICATIONS **629** CITATIONS

SEE PROFILE

Phys Chem Minerals (2001) 28: 167–176

ORIGINAL PAPER

J. Tangeman · D. Xirouchakis

High-temperature heat capacity and thermodynamic properties for end-member titanite ($CaTiSiO_5$)

Received: 30 December 1999 / Accepted: 23 June 2000

Abstract The heat capacity of end-member titanite and ($CaTiSiO_5$) glass has been measured in the range 328–938 K using differential scanning calorimetry. The data show a weak λ-shaped anomaly at 483 ± 5 K, presumably associated with the well-known low-pressure $P2_1/a \leftrightarrow A2/a$ transition, in good agreement with previous studies. A value of 0.196 ± 0.007 kJ mol^{-1} for the enthalpy of the $P2_1/a \leftrightarrow A2/a$ transition was determined by integration of the area under the curve for a temperature interval of 438–528 K, bracketing the anomaly. The heat capacity data for end-member titanite and ($CaTiSiO_5$) glass can be reproduced within <1% using the derived empirical equations (temperature in K, pressure in bars):

$$C_p^{\text{glass}} = \frac{114.7155 \times 10^6}{T^3} + \frac{-908.3 \times 10^{-3}}{T^2} + \frac{0.3170 \times 10^5}{T} + \frac{-0.8484 \times 10^4}{\sqrt{T}} + 0.5796 \times 10^3 + (-21.75) \times 10^{-2}\, T + 7.8731 \times 10^{-5}\, T^2 \quad (1)$$

$$C_p^{\text{solid}} = \frac{-2.3952 \times 10^6}{T^3} + \frac{-5.8601 \times 10^{-3}}{T^2} + \frac{0.2239 \times 10^5}{T} + \frac{-0.5913 \times 10^4}{\sqrt{T}} + 0.4277 \times 10^3 + (-7.772) \times 10^{-2}\, T + 1.3751 \times 10^{-5}\, T^2 + 3.0877 \sum_{1}^{k=2} \frac{\tau^{3\cdot(2k-1)}}{2k-1} \quad \text{for } \tau = \frac{T}{T_{\text{transition}}} \leq 1 \quad \text{or } 2.3034 \sum_{1}^{k=2} \frac{\tau^{-5\cdot(2k-1)}}{2k-1} \quad \text{for } \tau = \frac{T}{T_{\text{transition}}} \geq 1 \quad (2)$$

The available enthalpy of vitrification (80.78 ± 3.59 kJ mol^{-1}), and the new heat capacity equations for solid and glass can be used to estimate (1) the enthalpy of fusion of end-member titanite (122.24 ± 0.2 kJ mol^{-1}), (2) the entropy of fusion of end-member titanite (73.85 ± 0.1 J/mol K^{-1}), and (3) a theoretical glass transition temperature of 1130 ± 55 K. The latter is in considerable disagreement with the experimentally determined glass transition temperature of 1013 ± 3 K. This discrepancy vanishes when either the adopted enthalpy of vitrification or the liquid heat content, or both, are adjusted.

Calculations using Eq. (2), new P–V–T data for titanite, different but also internally consistent thermodynamic data for anorthite, rutile, and kyanite, and experimental data for the reaction: anorthite + rutile = titanite + kyanite strongly suggest: (1) the practice to adjust the enthalpy of formation of titanite to fit phase equilibrium data may be erroneous, and (2) it is probably the currently accepted entropy of 129.2 ± 0.8 J/mol K^{-1} that may need revision to a smaller value.

Key words Titanite · Heat capacity · Enthalpy · Entropy · Lambda transition

J. Tangeman (✉)[1]
Department of Geological Sciences,
2534 C.C. Little Building, University of Michigan,
Ann Arbor, Michigan 48109-1063

D. Xirouchakis
Earth Sciences and Solar System Exploration Division,
NASA Lyndon B. Johnson Space Center,
Mail Code SN2, Houston, Texas 77058, USA
Tel.: +1-281-4835148; Fax: +1-281-4831573
e-mail: dxirouch@ems.jsc.nasa.gov

Present address:
[1] Thermochemistry Facility,
Department of Chemical Engineering and Materials Science,
University of California Davis, Davis CA 95616-8779, USA
Tel.: +1-530-7542132; Fax: +1-530-7529307
e-mail: jatangeman@ucdavis.edu

Introduction

Titanite is a common accessory mineral, probably the most common titanium-bearing mineral besides rutile and ilmenite, in igneous, metamorphic, and sedimentary rocks. Interest in its stability and crystal chemistry has been virtually constant among geologists and materials scientists since the the late 1920s (e.g., Zachariassen 1930; Fukusima 1936; Prince 1945; De Vries et al. 1955; Robbins 1968; Brower and Robbins 1969; Franz and Spear 1985; Crowe et al. 1986; Tanaka et al. 1988; Hayward et al. 1990; Cerny et al. 1995). Several studies have demonstrated its significance in petrology and glass/ceramics (e.g., Hunt and Kerrick 1977; Hayward and Cechetto 1982; Wones 1989; Xirouchakis and Lindsley 2000). Because of efforts to better understand the stability of titanite in natural and synthetic systems (e.g., Manning and Bohlen 1991; Xirouchakis and Lindsley 1998a, b), the interest in the thermodynamic properties of this mineral has been rekindled (e.g., Xirouchakis et al. 1997a, b; Thiéblot et al. 1999; Hayward et al. 2000).

In this study, we use well-characterized, synthetic samples and differential scanning calorimetry to obtain the high temperature heat capacity of end-member titanite and glass of $CaTiSiO_5$ composition. Subsequently, we compare our data with those from other studies, and we discuss the implications to the thermodynamic data for titanite. Note that the samples used in this study had been previously employed to redetermine the unit cell volume, enthalpy of formation of end-member titanite and $CaTiSiO_5$ glass, and to study the $P2_1/a \leftrightarrow A2/a$ transition in situ at high pressures (Kunz et al. 1996; Xirouchakis et al. 1997a, b; Angel et al. 1999; Kunz et al. in prep.).

Previous Work

King et al. (1954) were the first to investigate the thermodynamic properties of crystalline titanite and $CaTiSiO_5$ liquid. According to King et al. (1954), the crystalline sample contained at least 1% impurities that they did not identify. King et al. (1954) performed low-temperature adiabatic calorimetry from 50 to 298 K, and heat content measurements from 400 to 1800 K. Subsequently, they estimated a value of 129.2 ± 0.84 J mol^{-1} K^{-1} for $S^\circ_{1\,\mathrm{bar},298\,\mathrm{K}}$. Todd and Kelley (1956) used the same sample and hydrofluoric (HF) calorimetry at 74 °C to obtain the enthalpy of formation at 25 °C. These authors give -112.34 ± 1 kJ mol^{-1} as the enthalpy of formation from the oxides, which corresponds to -2602.8 ± 2.1 kJ mol^{-1} from the elements. Surprisingly, in the same study, the enthalpy of formation from the elements is also given as -2564.4 ± 4.6 kJ mol^{-1}. The reasons behind this discrepancy are not understood. Based upon those earlier studies, Robie et al. (1978) accepted -2601.4 ± 2.4 kJ mol^{-1} as the enthalpy of formation from the elements and 129.20 ± 0.84 J mol^{-1} K^{-1} as the entropy at 25 °C and 1 bar. Robie and Hemingway (1995) adjusted the enthalpy of formation to -2595 ± 3 kJ mol^{-1} to better agree with the results from thermodynamic modeling of titanite-bearing phase equilibrium experiments (Berman 1988; Holland and Powell 1990).

New high-temperature (975 K) drop-solution calorimetry measurements demonstrated the need for revision of the enthalpy of formation of titanite (Xirouchakis et al. 1997b). In addition, Xirouchakis and Lindsley (1998a) suggested that the currently available heat capacity and standard entropy may require revision. They also demonstrated that, (1) an enthalpy of formation value of -2610 ± 2.9 kJ mol^{-1} is consistent with entropy values either smaller than 110 J mol^{-1} K (Berman 1991) or 120 J mol^{-1} K^{-1} (Holland and Powell 1990) and (2) entropy values close to 129.20 J mol^{-1} K^{-1} (King et al. 1954) are consistent with enthalpy of formation values ≥ -2597 kJ mol^{-1} (Holland and Powell 1990; Berman 1991; Xirouchakis and Lindsley 1995) or ≥ -2602 kJ mol^{-1} (Holland and Powell 1985). Independent support for these conclusions comes from the recent work of Holland and Powell (1998) and Chatterjee et al. (1998). For instance, Holland and Powell (1998) evaluated the $\Delta H^\circ_{1\,\mathrm{bar},298\,\mathrm{K}}$ and $S^\circ_{1\,\mathrm{bar},298\,\mathrm{K}}$ for titanite as -2596 ± 1.04 kJ mol^{-1} and 131.20 J mol^{-1} K^{-1}, respectively, whereas Chatterjee et al. (1998) derived an enthalpy of formation from the elements for titanite of -2594 ± 0.7 kJ mol^{-1} for a standard entropy of 129.20 ± 0.6 J mol^{-1} K^{-1}.

If the Todd and Kelley (1956) data are corrected for phase impurities [see below Eq. (5)]: $CaTiSiO_5$ glass, quartz or other SiO_2 polymorphs, wollastonite, and rutile, the enthalpy of formation changes to values more negative than -2602.8 kJ mol^{-1}. Depending upon assumptions regarding the proportions of phase impurities, the enthalpy of formation can range from -2604 to -2619 kJ mol^{-1}, in better agreement with the more negative value of -2610.13 ± 2.90 kJ mol^{-1} (Xirouchakis et al. 1997b). Hence an enthalpy of formation value of ≥ -2605 kJ mol^{-1} is deemed more appropriate for the Todd and Kelley sample. At 975 K titanite has the high-temperature structure ($A2/a$) vs. the low-temperature structure ($P2_1/a$) at 74 °C. Conceivably, this may have contributed to the Xirouchakis et al. (1997b) data. However, such a contribution is likely within the experimental uncertainty.

Zhang et al. (1995) presented, as a figure, heat-capacity data obtained with a differential scanning calorimeter in the range 350 to 940 K. The Zhang et al. (1995) sample came from a single crystal with a suspiciously large unit cell that also contains phase impurities, presumably $CaSiO_3$ and SiO_2 (Tanaka et al. 1988). Chrosch et al. (1997), however, claimed that the Zhang et al. (1995) sample did not appear to contain any defects. Zhang et al. (1995) identified a λ-shaped heat capacity anomaly at 486 K, where the $P2_1/a \pm A2/a$ transition in titanite is known to take place at room

pressure, cf. 496 ± 20 K (Taylor and Brown 1976). Moreover, Zhang et al. (1995) proposed that a second high-temperature transition is possible at 850 ± 50 K. Finally, Thiéblot et al. (1999) measured the heat content of a polycrystalline titanite ($CaTiSiO_5$) sample with a unit cell volume of 369.43 ± 0.35 Å^3 and not 368.6 Å^3 (Thiéblot et al. 1999). No microprobe data are reported. Thiéblot et al. (1999) derived heat-capacity equations from fitting the high-temperature heat-content data. As for $CaTiSiO_5$ glass, no actual heat-capacity data are available.

Experimental procedures

Sample synthesis and characterization

The $CaTiSiO_5$ glass (sample no: glass 96) was obtained as follows. First, a $CaCO_3$-TiO_2-SiO_2 mixture was decarbonated by raising the temperature from 500 to 1000 °C over a period of 75 h and at 1050 °C for 3 days. Subsequently, the mixture was melted in a Pt crucible at 1400 °C for 24 h. The sample was brought from red heat to below incandescent temperature within 60 s by immersing the Pt crucible in water. The product was a transparent and clear glass. The only apparent flaw, observed at the surface of the bulk material and in contact with the Pt crucible, was a small, ≤2 mm^2, circular milky white area. Optical examination and powder X-ray diffraction (Cu Kα radiation), before and after drying at 200 °C for 10 h, indicate that it is isotropic and does not contain any crystals. All the available observations and analyses strongly indicate a homogeneous, pure $CaTiSiO_5$ glass (Xirouchakis 1997b).

Titanite sample 96-2 was synthesized by annealing a portion of the above glass sample at 1100 °C for 5 days and 24 h at 1050 °C with two cycles of thorough grinding in between. The crystalline sample 96-1 was synthesized by reacting in a Pt crucible an equimolar mechanical mixture of $CaSiO_3$-TiO_2 at 1100 °C for 14 days and 1200 °C for 21 days with 2–3 h of grinding between annealing periods. Crystalline sample 96-2 lacks phase impurities whereas several titanite grains in sample 96-1 were found to contain unreacted cores of $CaSiO_3$ and SiO_2. However, samples 96-1 and 96-2 are both stoichiometric and appear nearly identical within the resolution of the techniques that have been studied (Xirouchakis et al. 1997a, b).

In contrast, sample 93-1 is nonstoichiometric, and possibly Si-deficient, with small amounts of Ca-, and Si-rich impurities (Xirouchakis et al. 1997a). In addition, it has a larger unit cell (Table 1) and a statistically different enthalpy of formation (Xirouchakis et al. 1997a) than the stoichiometric samples 96-1 and 96-2. Sample 93-1 was synthesized by annealing a phase pure glass sample with the desired composition, but also milky white in appearance, for 48 h at 1100 °C with two cycles of grinding (details in Xirouchakis et al. 1997a, b).

To maintain internal consistency, unit cell parameters for all samples were re-determined using the same diffractometer and the same procedure. Powder X-ray diffraction data were collected using a Philips diffractometer equipped with incident soller slits, θ compensating slit, a graphite monochromator, a scintillation detector, and CuKα radiation in steps of 0.02° 2θ at a rate of 2 s per step. Intensity data measured as relative peak heights above background of hand-picked peaks were obtained using the Siemens IFFRAC5000 second derivative peak locate program. The positions were then corrected using SRM 660, LaB_6, as an external calibrant. Least-squares refinement of the lattice parameters was performed using the least-squares program NBSLSQ (Hubbard et al. 1985). Casual inspection of the unit cell parameters for titanite samples 96-1 and 93-1 reported in Table 1 and in Xirouchakis et al. (1997a) reveals good agreement for sample 96-1 between the two studies. However, there are differences in the unit cell parameters of the nonstoichiometric sample 93-1, specifically in the a-axis and consequently the unit cell volume. The reasons for this discrepancy may be possibly traced to the smaller quantity of 93-1 available for powder XRD, approximately 50% less, relative to 96-1 and 96-2. Alternatively, it may relate to the finer grain size used by Xirouchakis et al. (1997a). All powdered samples in the latter study were obtained by selecting the particles remaining suspended after 2 min of sedimentation in alcohol.

Heat capacity measurements

High-temperature heat capacities were measured with a power-compensated differential scanning calorimeter (Perkin-Elmer DSC-7) at the University of Michigan. The temperature was calibrated against the melting points of indium (429.75 K) and zinc (692.55 K). Measurements were performed in a dry air atmosphere with a flow rate of 30 cc min^{-1}. The samples were loaded into gold pans and data were collected at intervals of 10° using a heating rate of 10 K min^{-1}. Results for each sample were calibrated with the NBS-720 (pure α-Al_2O_3) standard (Ditmars and Douglas 1971). The heat capacities were then derived using the method of Mraw (1988). Corrections for differences in pan weights were made using the heat capacity for gold (Robie and Hemingway 1995). Analyses of single crystal periclase (MgO) were used to assess the accuracy and reproducibility of the DSC scans. These scans served effectively as a standard for inter- and intra-laboratory comparison. Agreement between our curve fitted through five periclase scans performed over the same period of time during which the titanite data were collected and the fitted curve of Robie and Hemingway (1995) for periclase is excellent, with a maximum discrepancy of 0.8%. Reproducibility of the C_P data for periclase is generally better than 1% over the entire temperature range. Several scans were performed for each sample and the mean was taken as the final value with one standard deviation less than or equal to the precision of the method (1%) (Tangeman 1998; Tangeman and Lange 1998). The glass transition temperature of the glass sample (glass 96) in

Table 1 Titanite unit cell parameters at atmospheric conditions of samples either referred to or used in this study. *Numbers in parentheses and brackets* refer to the last digit(s) and are 1σ deviations. *Numbers in brackets* were calculated propagating the errors in the unit cell parameters

Sample	a (Å)	b (Å)	c (Å)	b (°)	V (Å^3)
Ttn 93-1[a]	7.074 (1)	8.725 (1)	6.568 (1)	113.87 (1)	370.71 (11)
Ttn 96-1[b]	7.061 (1)	8.713 (1)	6.558 (0)	113.81 (1)	369.13 (4)
Ttn 96-2[b]	7.061 (1)	8.715 (0)	6.561 (0)	113.82 (1)	369.39 (7)
Thiéblot et al. (1999)[c]	7.065 (5)	8.720 (5)	6.557 (4)	113.86 (5)	369.43 (35)
Tanaka et al. (1988)[b]	7.081 (4)	8.736 (3)	6.569 (3)	113.89 (4)	371.54 (1.01)
Manning and Bohlen (1991)[a]	7.065 (3)	8.719 (4)	6.562 (3)	113.84 (4)	369.7 (5)

[a] Nonstoichiometric
[b] Stoichiometric
[c] Stoichiometry unknown

this study was determined using a Netzsch DSC-404 at the University of California, Davis. The glass sample, in powder form, was scanned at a rate of 10 K min^{-1} with Ar as the purge gas flowing at 30 cc min^{-1}.

Discussion

Heat capacity

The results for all samples are presented in Table 2, where the average heat capacity data of polycrystalline samples 96-1 and 96-2 are also included. We consider these average C_P data as the best representative of stoichiometric, phase-pure titanite ($CaTiSiO_5$). No major differences are readily distinguished among the heat capacity data of the stoichiometric and nonstoichiometric titanite (Table 2; Fig. 1). However, the specific heat data of the nonstoichiometric sample (93-1) generally have larger errors associated with them and plot lower than the data for the end-member titanite, consistent with the presence of phase impurities, and nonstoichiometry.

Our heat-capacity data for end-member titanite (average of samples 96-1 and 96-2) compare reasonably well with the Zhang et al. (1995) data only up to 700 K. At higher temperatures our measurements differ from the Zhang et al. data between +1.5 and +4 J mol^{-1} K (Fig. 1). Note that we scanned the Zhang et al. (1995) data from their Fig. 9. In addition, the anomaly peak shape in the Zhang et al. (1995) data is sharp relative to the broad, rounded peaks shown by our C_P curves. Nevertheless, in our data, the maximum C_P and the corresponding change in slope of the C_P curve in the region of the anomaly occurs at 483 ± 5 K, similar to the transition temperature of 486 K reported by Zhang et al. (1995). The difference in the shape of the transition between our C_P curves and that shown by the Zhang et al. (1995) data is most likely due to the difference in the nature of the samples. Although not entirely clear from the description, Zhang et al. (1995) appear to have used a piece of a single crystal of titanite, whereas our samples are polycrystalline powders.

The enthalpy of transition in this study was determined by fitting a Haas and Fisher (1976) equation through the sets of data for a particular sample over the entire temperature range of the C_P curve and then integrating the area bounded by the fitted curve and the experimental data over a 10° temperature interval bracketing the transition peak for that sample. The enthalpy of transition determined for the titanite samples in this study is 0.196 ± 0.007 kJ mol^{-1}, which is substantially lower than the ΔH_{trans}^{Ttn} of 0.342 kJ mol^{-1} obtained using the same method for the Zhang et al. (1995) data. The difference in the enthalpy of transition between the two studies is probably due to the different grain sizes of the samples. Furthermore, this difference is consistent with the observations of Ghiorso et al. (1979) for the $\alpha \leftrightarrow \beta$ transition in quartz. They found that $\Delta H_{trans}^{\alpha \leftrightarrow \beta Qz}$ obtained over 9° from DSC runs is dependent upon the sample grain size; for a crushed powder, $\Delta H_{trans}^{\alpha \leftrightarrow \beta Qz}$ is 384.93 ± 5.86 J mol^{-1} whereas for a single piece of quartz, $\Delta H_{trans}^{\alpha \leftrightarrow \beta Qz}$ is 450.62 ± 5.86 J mol^{-1}. The ΔH_{trans}^{Ttn} of 0.196 ± 0.007 kJ mol^{-1} is higher than that reported by Thiéblot et al. (1999) of ~0.080 kJ mol^{-1}; however, it is not clear how the enthalpy for the $P2_1/a \leftrightarrow A2/a$ transition was determined in that study. The data reported herein cannot offer a clear indication whether a second transition exists at 850 ± 50 K (Zhang et al. 1995, 1997; Chrosch 1997).

The data for ($CaTiSiO_5$) glass, and end-member titanite (average of stoichiometric samples 96-2 and 96-1) were fitted with the Hemingway and Haas (1992) empirical equation which resulted in the following expressions:

$$C_p^{glass} = \frac{114.7155 \times 10^6}{T^3} + \frac{-908.3 \times 10^{-3}}{T^2} + \frac{0.3170 \times 10^5}{T} + \frac{-0.8484 \times 10^4}{\sqrt{T}} + 0.5796 \times 10^3 + (-21.75) \times 10^{-2}\, T + 7.8731 \times 10^{-5}\, T^2 \quad (3)$$

$$C_p^{solid} = \frac{-2.3952 \times 10^6}{T^3} + \frac{-5.8601 \times 10^{-3}}{T^2} + \frac{0.2239 \times 10^5}{T} + \frac{-0.5913 \times 10^4}{\sqrt{T}} + 0.4277 \times 10^3 + (-7.772) \times 10^{-2}\, T + 1.3751 \times 10^{-5}\, T^2 + 3.0877 \sum_{1}^{k=2} \frac{\tau^{3\cdot(2k-1)}}{2k-1} \quad \text{for } \tau = \frac{T}{T_{transition}} \le 1 \quad \text{or } 2.3034 \sum_{1}^{k=2} \frac{\tau^{-5\cdot(2k-1)}}{2k-1} \quad \text{for } \tau = \frac{T}{T_{transition}} \ge 1 \ . \quad (4)$$

At high temperature, practically above 2000 K, the heat capacity of the solid was constrained to approach the Dulong-Petit limit of $3 \cdot n \cdot R + a^2 \cdot T \cdot V/b$ (Berman and Brown 1985). The compressibility and thermal expansivity for titanite were derived by fitting the data of Taylor and Brown (1976), Angel et al. (1999), and Kunz et al. (in prep.) simultaneously. Equations (3) and (4) reproduce the data within experimental error and with an absolute average deviation less than or equal to 0.2% (Figs. 2, 3).

Relative to our C_P data for end-member titanite, the calculated King et al. (1954) and Thiéblot et al. (1999) C_P data appear to underestimate the titanite heat capacity of the $A2/a$ phase but also may slightly overestimate the heat capacity of the $P2_1/a$ phase (Fig. 2). King et al. (1954) established the heat capacity by combining their low-temperature adiabatic calorimetry and high-temperature heat-content data. They also estimated the impurity content in their sample as 1%. The nature of the impurities is unknown, e.g., Ca_2SiO_4 versus $CaSiO_3$ or titanite glass or other calc-silicate and silica phases. In addition to the phase impurities and perhaps because of them, the King et al. (1954) titanite

Table 2 High-temperature, experimental specific heat data of polycrystalline samples 96-2, 96-1, and 93-1, and glass sample 96. C_P units are J mol^{-1} K^{-1}. n is the number of scans per sample

T (K)	Ttn 96-1		Ttn 96-2		96-1 & 96-2		Ttn 93-1		glass 96	
	(n = 6)	(1σ)	(n = 6)	(1σ)	(n = 12)	(1σ)	(n = 6)	(1σ)	(n = 7)	(1σ)
328	145.5	0.4	146.9	1.3	146.2	0.8	144.6	0.2	147.5	0.5
338	148.7	0.6	149.4	1.0	149.0	0.8	148.3	1.2	149.9	0.5
348	150.9	0.6	151.7	1.0	151.3	0.8	150.6	1.0	152.0	0.5
358	153.0	0.9	153.9	1.2	153.5	1.1	152.7	1.1	154.2	0.5
368	155.2	0.7	156.0	1.0	155.6	0.9	155.0	1.0	156.1	0.5
378	157.2	0.8	158.0	0.9	157.6	0.9	156.7	0.9	157.8	0.4
388	159.3	0.8	160.0	0.9	159.6	0.9	158.7	0.9	159.8	0.4
398	161.2	0.9	161.9	1.0	161.5	0.9	160.8	1.0	161.6	0.5
408	162.9	0.8	163.6	0.9	163.3	0.9	162.5	1.0	163.1	0.4
418	164.7	0.8	165.4	0.8	165.0	0.8	164.3	0.9	164.7	0.5
428	166.4	0.9	167.2	1.0	166.8	0.9	166.1	1.0	166.3	0.4
438	168.2	0.9	168.9	1.1	168.6	1.0	168.2	1.1	167.7	0.5
448	169.9	0.9	170.5	1.0	170.2	1.0	169.8	0.9	169.0	0.5
458	171.7	0.9	172.1	1.0	171.9	1.0	171.6	1.0	170.4	0.5
468	173.8	0.9	173.6	1.0	173.7	0.9	173.6	1.2	171.9	0.4
478	175.9	0.9	174.6	1.3	175.3	1.1	175.1	0.5	172.7	0.3
488	175.2	1.2	175.0	1.4	175.1	1.3	175.0	0.6	174.0	0.4
498	176.1	1.3	175.8	1.4	175.9	1.3	175.4	1.2	175.1	0.7
508	176.1	0.7	176.6	1.4	176.3	1.1	176.0	1.6	176.3	0.6
518	176.5	0.7	177.4	1.3	177.0	1.0	175.9	0.9	177.3	0.5
528	177.4	0.7	178.4	1.3	177.9	1.0	176.9	0.9	178.4	0.5
538	178.2	0.7	179.2	1.5	178.7	1.1	177.6	1.2	179.4	0.5
548	178.9	0.7	179.8	1.3	179.3	1.0	178.2	1.0	180.0	0.5
558	179.7	0.8	180.7	1.3	180.2	1.1	179.2	0.9	181.2	0.5
568	180.4	0.7	181.6	1.4	181.0	1.0	180.0	1.0	182.0	0.4
578	181.2	0.8	181.8	0.9	181.5	0.8	180.7	1.0	182.9	0.6
588	181.7	0.6	182.5	0.7	182.1	0.7	181.3	1.0	183.5	0.6
598	182.4	0.6	183.5	0.5	182.9	0.6	182.1	1.0	184.5	0.4
608	183.3	0.5	184.3	0.8	183.8	0.7	182.9	1.0	185.1	0.5
618	183.7	0.4	184.8	0.6	184.2	0.5	183.6	1.1	185.5	0.6
628	184.2	0.5	185.5	0.7	184.9	0.6	184.2	1.0	186.3	0.7
638	184.7	0.6	186.2	0.9	185.4	0.7	184.9	1.1	187.1	0.8
648	185.1	0.7	186.6	0.7	185.8	0.7	185.4	1.2	187.7	0.8
658	185.6	0.7	187.1	0.5	186.4	0.6	185.8	1.0	188.2	0.9
668	186.5	0.6	187.7	0.6	187.1	0.6	186.5	1.2	188.9	0.7
678	187.0	0.8	188.2	0.8	187.6	0.8	187.0	1.2	189.6	0.9
688	187.4	0.7	188.7	0.7	188.0	0.7	187.5	1.2	190.1	0.9
698	188.0	0.6	189.2	0.6	188.6	0.6	187.9	1.0	190.8	0.6
708	188.5	0.9	190.0	1.0	189.2	0.9	188.4	1.4	191.3	0.8
718	189.1	0.6	190.3	0.8	189.7	0.7	189.0	1.4	192.0	0.9
728	189.4	0.6	190.9	0.7	190.2	0.7	189.3	1.4	192.3	0.7
738	190.0	0.7	191.3	0.8	190.6	0.8	189.9	1.3	193.1	0.7
748	190.5	0.7	191.8	1.1	191.1	0.9	190.4	1.4	193.5	0.9
758	190.8	0.7	192.2	0.9	191.5	0.8	190.8	1.4	194.0	1.0
768	191.3	0.8	192.8	1.0	192.1	0.9	191.2	1.4	194.6	0.8
778	191.6	0.9	193.1	1.2	192.4	1.1	191.7	1.5	195.0	1.1
788	191.9	0.8	193.4	1.2	192.7	1.0	192.0	1.5	195.5	1.1
798	192.3	0.8	194.0	1.1	193.1	1.0	192.3	1.2	195.9	1.1
808	192.8	0.6	194.4	1.4	193.6	1.0	192.8	1.5	196.5	0.9
818	193.0	0.8	194.9	1.3	194.0	1.1	193.0	1.6	196.6	0.9
828	193.3	1.0	195.3	1.4	194.3	1.2	193.5	1.5	197.0	1.3
838	194.1	0.8	195.7	1.4	194.9	1.1	193.8	1.4	197.8	0.9
848	194.0	1.0	195.8	1.1	194.9	1.0	194.4	1.4	197.8	1.2
858	194.4	1.0	196.3	1.2	195.4	1.1	195.3	1.2	198.0	1.5
868	194.5	0.8	196.6	1.0	195.6	0.9	195.8	1.4	198.2	1.4
878	194.9	0.9	197.0	1.4	196.0	1.1	195.8	1.5	199.2	1.1
888	195.3	1.0	197.2	1.6	196.3	1.3	196.1	1.7	199.6	1.4
898	195.4	1.0	197.6	1.4	196.5	1.2	196.4	1.2	200.0	1.4
908	195.9	0.8	198.0	1.5	197.0	1.2	197.0	1.6	200.7	1.5
918	196.5	1.0	198.3	1.9	197.4	1.5	197.5	1.9	201.1	1.4
928	196.0	1.0	198.0	1.4	197.0	1.2	197.4	1.6	201.2	1.4
938	196.4	0.9	199.1	1.4	197.8	1.1	197.3	1.2	201.8	1.3
948							196.8	0.3	201.0	0.0

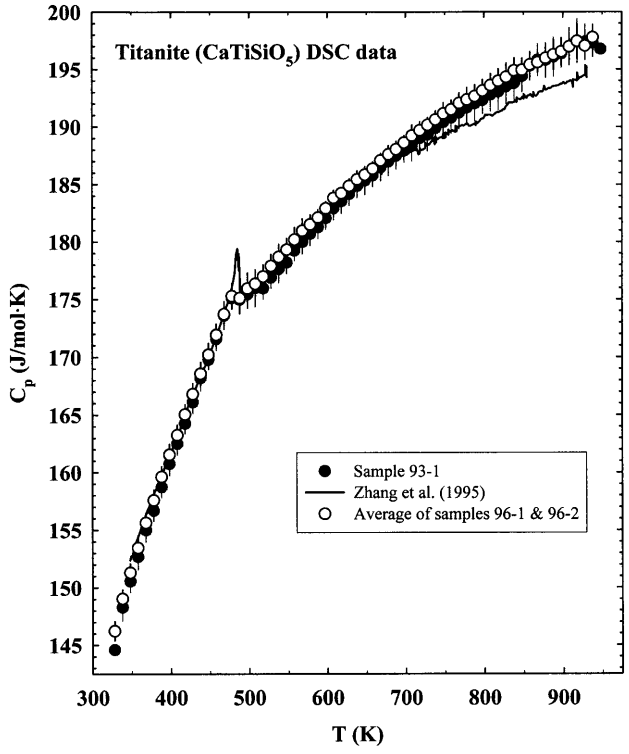

Fig. 1 Heat capacity of the titanite samples vs. T plot. *Error bars* (1σ) are equal to or smaller than the size of symbols unless shown otherwise. *Heavy solid line* represents the data of Zhang et al. (1995)

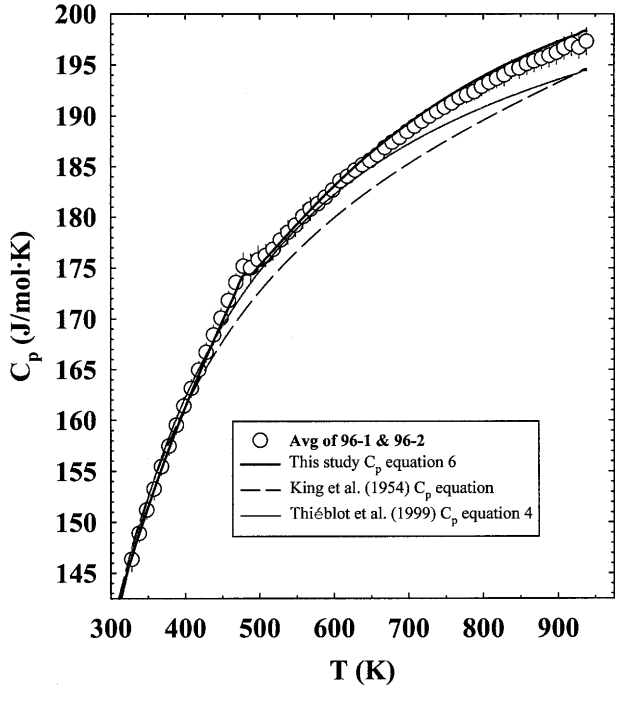

Fig. 2 Heat capacity of end-member titanite vs. T plot. *Error bars* (1σ) are equal to or smaller than the size of symbols unless shown otherwise. *Heavy solid line* represents fit to the data with Eq. (6). *Heavy dark gray line* is calculated with Eq. (4) of Thiéblot et al. (1999). *Dashed heavy line* is calculated with the King et al. (1954) equation

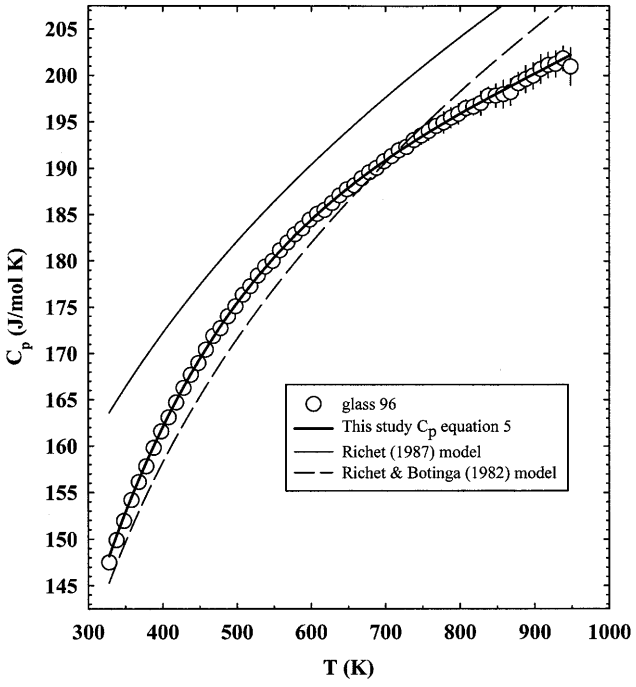

Fig. 3 Heat capacity of sample $CaTiSiO_5$ glass vs. T plot

sample may have a greater number of lattice imperfections. The latter may also contribute to the measured thermodynamic quantities by increasing the entropy of the crystals. For simplicity, we can assume that only phase impurities contribute to the C_P and that they are a $CaSiO_3$ or SiO_2 phase, $CaTiSiO_5$ glass, or all of the above. Subsequently, we can evaluate their effect through the relation:

$$Y^{\text{corrected}} = \frac{Y^{\text{measured}} - \sum_1^i x_i \cdot Y_i^{\text{other}}}{1 - \sum_1^i x_i} \quad , \tag{5}$$

where $\sum_1^i x_i$ represents the amount of other phases. This correction can result in an overall increase to the King et al. (1954) heat content and specific heat, bringing the latter into agreement with this study, especially at high temperatures. Finally, we compare the $CaTiSiO_5$ glass heat-capacity data to the Richet and Bottinga (1982) and Richet (1987) model predictions. Only the Richet and Bottinga (1982) model compares favorably with our data (Fig. 3).

Heat content

We use Eq. (4) to calculate the heat content of end-member titanite and compare them to the King et al. (1954) and Thiéblot et al. (1999) experimental data (Fig. 4A). Relative to our calculated heat-content data, the Thiéblot et al. (1999) measurements deviate positively from as high as 17% below 483 K to <1% at 1500 K. In contrast, the King et al. (1954) data deviate from our data positively by as much as 10% below, and negatively by 1–2% above 483 K. At temperatures close

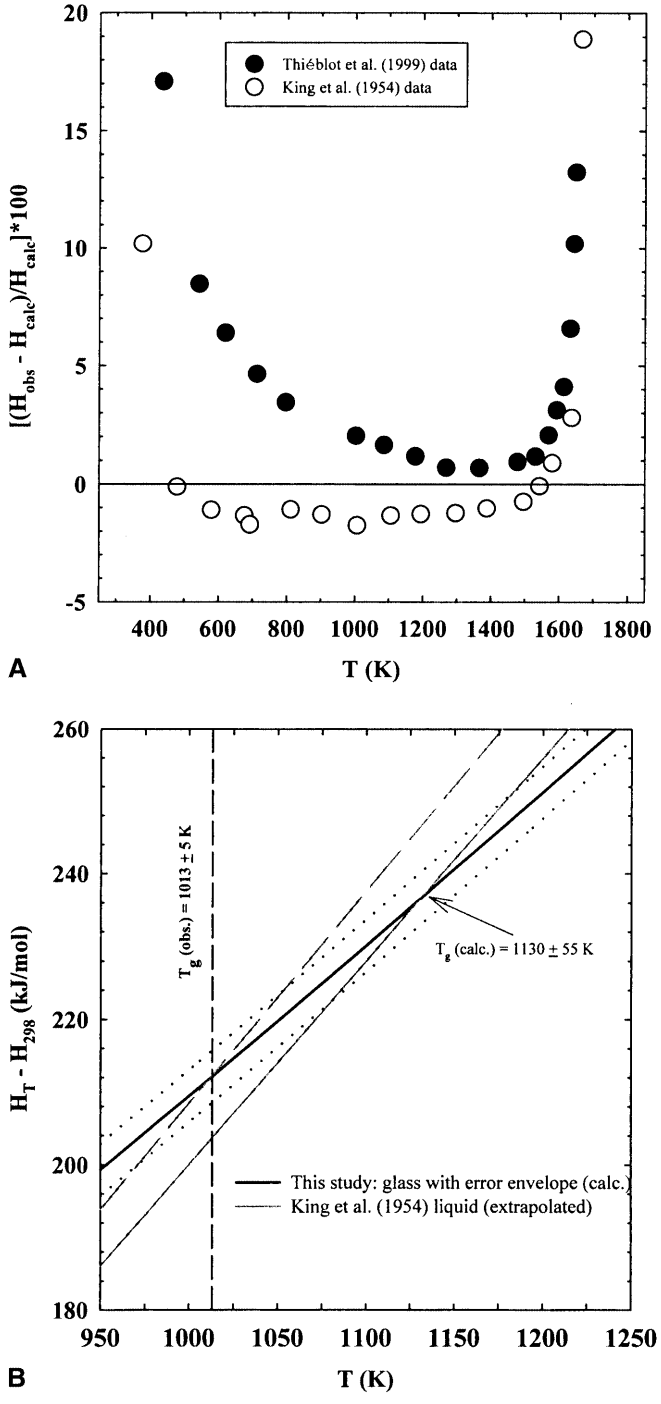

Fig. 4 **A** Percent heat content deviations as a function of T. The observed heat content data are from the actual King et al. (1954) and Thiéblot et al. (1999) measurements. The calculated heat content data are computed after integration of Eq. (4) in the interval 298–1900 K. **B** Glass and liquid heat content as a function of temperature, and the calculated vs. observed glass transition temperature for the fast quenched $CaTiSiO_5$ glass sample of this study. The glass heat content is calculated using Eq. (3) after integration (298–1800 K), whereas the liquid heat content is calculated with the equation given by King et al. (1954) for the same T range. *Dashed gray line* represents the average adjustment to the liquid heat content within the 2.5 to 5.9% range in order to make the calculated glass transition T agree with the observed one

to the melting point (1655 ± 5 K) and because of the effects of melting, both studies overestimate the heat content. The respective average deviations between our calculated heat content and the King et al. (1954) and Thiéblot et al. (1999) heat content measurements are +1.2 ± 0.8 and −2.6 ± 0.8 kJ mol^{-1}. At 975 K, and for a stoichiometric and phase-pure crystalline sample with a unit cell volume comparable to that of 96-2 and 96-1 (94-2: Xirouchakis et al. 1997a), there is an independent estimate of the heat content. A value of 122.985 ± 1 kJ mol^{-1} was obtained from the difference of drop solution and preliminary solution calorimetry experiments of titanite in $2PbO{\cdot}B_2O_3$ solvent (S. Fritsch 1995, written communication). This value compares better with the calculated heat content using Eq. (4) of this study (122.486 kJ mol^{-1}) and the Thiéblot et al. (1999) equations [e.g., Eq. (3): 121.724 kJ mol^{-1}] than the King et al. (1954) function (120.605 kJ mol^{-1}). The King et al. (1954) function reproduces the original data with an average deviation of less than 0.3%. Although a single measurement, we do not believe the agreement to be fortuitous, since all the stoichiometric and phase-pure titanite samples that we have synthesized have similar physicochemical characteristics, i.e., $V^{\circ}_{1\,\mathrm{bar},298\,\mathrm{K}}$, $C_P(T)$, $\Delta H^{\circ}_{1\,\mathrm{bar},298\,\mathrm{K}}$ Such agreement implies that the observed increase in our data, relative to the King et al. (1954) heat-content data is small but also real. Finally, we want to emphasize the fact that both studies appear to overestimate both the heat capacity and the heat content of the $P2_1/a$ phase. This may result in overestimating the S of end-member titanite, something that is discussed later in this paper.

Thermodynamic data for titanite ($CaTiSiO_5$)

To calculate the glass transition temperature, enthalpy of fusion, and entropy of fusion of end-member titanite, we adopted 80.78 ± 3.59 kJ mol^{-1} as the enthalpy of vitrification at 298 K (Xirouchakis et al. 1997b), 1655 ± 5 K as the melting temperature, and the $CaTiSiO_5$ liquid C_P of King et al. (1954). The melting temperature was established using differential thermal analysis (DTA) at room pressure by Crowe et al. (1986) and it is 15 K lower than the temperature proposed by King et al. (1954) but in better agreement with the Thiéblot et al. (1999) melting temperature of 1658 ± 5 K. As a result, the calculated glass transition temperature is 1130 ± 55 K. Agreement with the experimentally determined glass transition temperature of 1013 ± 5 K is reached either when the enthalpy of vitrification, that contributes to the glass heat content, is adjusted within experimental uncertainty or the extrapolated King et al. (1954) liquid heat content or both. The liquid heat content adjustment is within +2.5 to +5.9%, and it is much greater than the stated precision of 0.1% in the range 1670 to 1800 K. Therefore, either the uncertainty of the original liquid data is greater than assumed or the King et al. (1954) liquid heat content

equation cannot be used with confidence below 1670 K. Note that Thiéblot et al. (1999) encountered difficulties in measuring the heat content of the liquid because of its high fluidity. The enthalpy and entropy of fusion is estimated to be 122.24 ± 0.2 kJ mol^{-1} and 73.85 ± 0.1 J mol^{-1} K^{-1}, respectively (cf. 123.8 ± 0.4 kJ mol^{-1} and 74.10 ± 0.2 J mol^{-1} K^{-1} in King et al. 1954).

We also estimated an internally consistent range of $\Delta H^{\circ}_{1\,\mathrm{bar},298\,\mathrm{K}}$ and $S^{\circ}_{1\,\mathrm{bar},298\,\mathrm{K}}$ values for titanite ($P2_1/a$ structure) using (1) different internally consistent thermodynamic data bases (Berman 1991; Holland and Powell 1998), (2) Eq. (6), (3) new P–V–T data for titanite (Taylor and Brown 1976; Angel et al. 1999; Kunz et al., in preparation), and (4) the Manning and Bohlen (1991) data for the reaction:

$$\underset{\text{anorthite}}{CaAl_2Si_2O_8} + \underset{\text{rutile}}{TiO_2} = \underset{\text{kyanite}}{Al_2SiO_5} + \underset{\text{titanite}}{CaTiOSiO_4} \quad . \qquad (6)$$

This data set is particularly useful because virtually all the phases have end-member composition. We say virtually all, because of the apparent 5 ± 1% deficiency in Si^{4+} or Ti^{4+} excess in initial and final titanite compositions (Manning and Bohlen 1991). Thus, the activities of anorthite, kyanite, and rutile were set equal to 1 whereas the titanite activity was set equal to 0.95 (Manning and Bohlen 1991). Thermodynamic data for anorthite, kyanite, and rutile were taken from the internally consistent data bases of Berman (1991) and Holland and Powell (1998). We derived $C_P(T)$ and $V^{\circ}_{P,T}$ equations for titanite compatible with each database, taking into account the $P2_1/a \leftrightarrow A2/a$ transition, and finally feasible solutions based solely on the Manning and Bohlen (1991) phase-equilibrium constraints. Note that the currently available thermal expansion and compressibility parameters for titanite, which are constrained from thermodynamic modeling (e.g., Berman 1998, 1991) of low-pressure phase-equilibrium experiments (Hunt and Kerrick 1977), cannot predict the high-pressure volume data (Fig. 5). Manning and Bohlen (1991) reported very good agreement between their experiments and the calculated equilibrium position for this reaction using the Berman (1988) database, an agreement that would carry over to the Berman (1991) database also, as values for the relevant phases were unchanged. Regardless of the database used, and in order to maintain consistency with the end-member titanite model for each database, we had to increase the reported pressure by 250 and up to 650 bars for critical titanite growth experiments at 1000 and 1100 °C. This increase is higher than the reported pressure variations of ±100 bars. The adjustment in pressure conditions, however, indicates that (1) the currently available thermodynamic data are optimized from a database of titanite samples with properties similar to the Manning and Bohlen (1991) titanite sample, and (2) the use of a nonstoichiometric titanite may have shifted the equilibrium reaction boundary to slightly lower pressures. The feasible solutions are depicted in Fig. 6. For the Berman (1991) database, the acceptable $\Delta H^{\circ}_{1\,\mathrm{bar},298\,\mathrm{K}}$ and

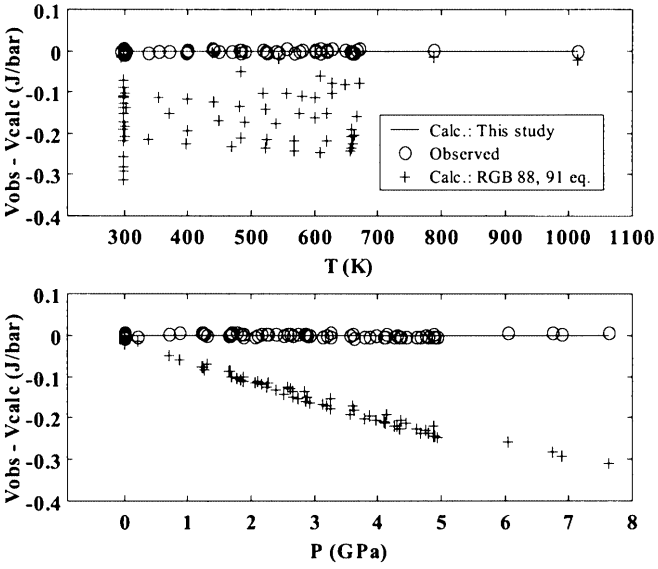

Fig. 5 ($V_{obs} - V_{calc}$) vs. T, and P plots. Use of the Holland and Powell (1990, 1998) volume equations produces similar results to the Berman (1998, 1991) equation

$S^{\circ}_{1\,\mathrm{bar},298\,\mathrm{K}}$ values for titanite are within −2591 to −2608 kJ mol^{-1} and 124 to 112 J mol^{-1} K^{-1}, respectively. For the Holland and Powell (1998) data base, the acceptable $\Delta H^{\circ}_{1\,\mathrm{bar},298\,\mathrm{K}}$ from the elements has to be ≤−2,600 kJ mol^{-1} whereas the acceptable $S^{\circ}_{1\,\mathrm{bar},298\,\mathrm{K}}$ is less than 120 J mol^{-1} K^{-1}. Clearly, regardless of the internally consistent data base or enthalpy of formation accepted, the entropy has to be revised to a value lower

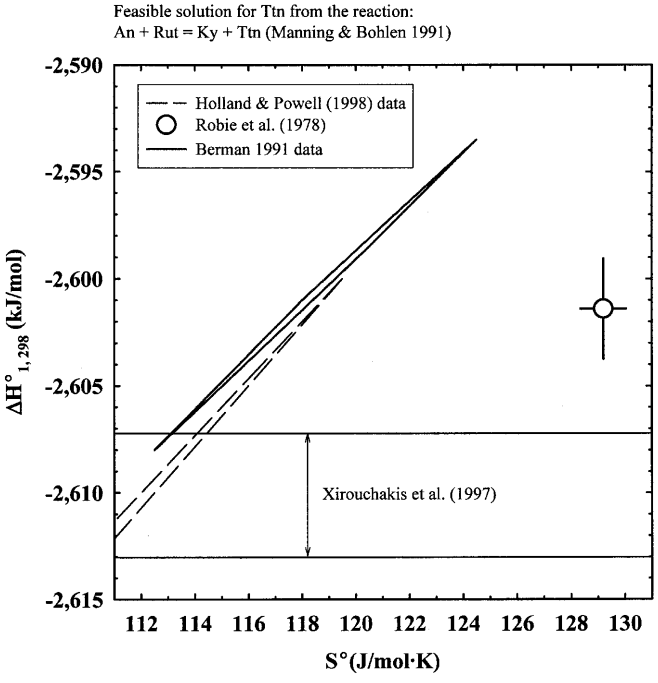

Fig. 6 Feasible solution for the reaction: anorthite + rutile = titanite + kyanite calculated using the internally consistent data bases of Berman (1991) and Holland and Powell (1998)

than 129.20 ± 0.84 J mol K^{-1} (Xirouchakis and Lindsley 1998a; Xirouchakis et al., unpublished manuscript). Of course, the actual value will depend on the thermodynamic data base of choice, i.e., Berman (1988, 1991); Andersen et al. (1993); Berman and Aranovich (1996); Holland and Powell (1990, 1998); Chatterjee et al. (1998).

Acknowledgements We wish to thank J.Y. Chan of the National Institute of Standards and Technology (NIST) for X-ray data collection and B. A. Reisner of the NIST Center for Neutron Research for X-ray data analysis, and I-Ching Lin for comments which improved the manuscript. Marc Hirschmann and Rebecca Lange provided encouragement and financial support through NSF grants OCE 971135, and EAR-9405678, respectively. The experiments at the Thermochemistry Facility at the University of California, Davis, were financially supported by A. Navrotsky through the Center for High Pressure Research (CHiPR), an NSF Science and Technology Center.

References

Andersen DJ, Lindsley DH, Davidson PM (1993) QUILF: a Pascal program to assess equilibria among Fe-Mg-Mn-Ti oxides, pyroxenes, olivine, and quartz. Comput Geosci 19, 9: 1333–1350

Angel RJ, Kunz M, Milletich P, Woodland BA, Koch M, Xirouchakis D (1999) High-pressure phase transition in titanite ($CaTiOSiO_4$). Phase Trans 68: 533–543

Berman RG, Brown TH (1985) Heat capacity of minerals in the system Na_2O-K_2O-CaO-MgO-FeO-Fe_2O_3-Al_2O_3-SiO_2-TiO_2-H_2O-CO_2: representation, estimation, and high temperature extrapolation. Contrib Mineral Petrol 89: 168–183

Berman RG (1988) Internally consistent thermodynamic data for minerals in the system Na_2O-K_2O-CaO-MgO-FeO-Fe_2O_3-Al_2O_3-SiO_2-TiO_2-H_2O-CO_2. J Petrol 29: 445–522

Berman RG (1991) Thermobarometry using multi-equilibrium calculations: a new technique, with petrological applications. Can Mineral 29: 833–855

Berman RG, Aranovich L (1996) Optimized standard state and solution properties of minerals. I. Model calibration for olivine, orthopyroxene, cordierite, garnet, and ilmenite in the system FeO-MgO-CaO-Al_2O_3-TiO_2-SiO_2. Contrib Mineral Petrol 126: 1–24

Brower WS, Robbins CR (1969) Growth of $CaTiSiO_5$ by the Czochralski method. J Crystallogr Growth 5: 233–234

Chatterjee NB, Krüger R, Haller G, Olbricht W (1998) The Bayesian approach to an internally consistent thermodynamic database: theory, database, and generation of phase diagrams. Contrib Mineral Petrol 133: 149–168

Cerny P, Novák M, Chapman R (1995) The Al (Nb, Ta) Ti_2 substitution in titanite: the emergence of a new species? Mineral Petrol 52: 61–73

Chrosch J, Bismayer U, Salje EKH (1997) Anti-phase boundaries and phase transitions in titanite: an X-ray diffraction study. Am Mineral 82: 677–681

Crowe MC, Greedan JE, Garrett JD, Burke NA, Vance ER, George IM (1986) Melt-grown sphene ($CaTiSiO_5$) crystals. J Mat Sci Lett 5: 979–980

De Vries RC, Ray R, Osborn EF (1955) Phase equilibria in the system CaO-TiO_2-SiO_2. J Am Ceram Soc 28: 158

Ditmars DA, Douglas TB (1971) Measurements of the relative enthalpy of pure α-Al_2O_3 (NBS Heat capacity and enthalpy reference material No. 720) from 273 to 1173 K. J Res 75A: 401–420

Franz G, Spear FS (1985) Aluminous titanite (sphene) from the eclogite zone, south-central Tauern Window, Austria. Chem Geol 50: 33–46

Fukusima IAM (1936) Metastable crystallization of $CaTiO_3$, TiO_2, SiO_2 in place of CaO-SiO_2-TiO_2 due to supercooling of the latter. Science Reports. Tohoku Imperial University Series 1, Honda Anniversary Volume, 454–464

Ghiorso MS, Carmichael ISE, Moret LK (1979) Inverted high-temperature quartz: unit cell parameters and properties of the _ ↔ _ inversion. Contrib Mineral Petrol 68: 307–323

Haas JL, Hemingway BS (1992) Recommended standard electrochemical potentials and fugacities of oxygen for solid buffers and thermodynamic data in the systems iron-silicon-oxygen, nickel-oxygen, and copper-oxygen. US Geol Surv Open File Rep, 92-267

Hayward SA, Del Cerro J, Salje EKH (2000) Antiferroelectric phase transition in titanite: excess entropy and short range order. Am Mineral 85: 557–562

Hayward PJ, Doern DC, George IM (1990) Dissolution of a sphene glass-ceramic, and of its component sphene and glass phases in Ca-Na-Cl brines. J Am Ceram Soc 73: 544–551

Hayward PJ, Cecchetto EV (1982) Development of sphene-based glass ceramics tailored For Canadian waste disposal conditions. In: Topp SJ (ed) The scientific basis for nuclear waste management, Elsevier, New York, pp 91–97

Holland TJB, Powell R (1998) An internally consistent thermodynamic data set for phases of petrological interest. J Metamorphic Geol 16, 3: 309–474

Holland TJB, Powell R (1990) An enlarged and updated internally consistent thermodynamic data set with uncertainties and correlations: the system Na_2O-K_2O-CaO-MgO-FeO-Fe_2O_3-Al_2O_3-SiO_2-TiO_2-C-H_2-O_2. J Metamorph Geol 8: 89–124

Hubbard CR, Lederman S, Pyrros NP (1985) NBSLSQ: a version of the geological survey lattice parameters least-squares program. National Bureau of Standards, Compiled for PC

Hunt JA, Kerrick DM (1977) The stability of sphene: experimental redetermination and geologic implications. Geochim Cosmochim Acta 41: 279–288

King EG, Orr RB, Bonnickson KR (1954) Low-temperature heat capacity, entropy at 298.16 K, and high-temperature heat content of sphene ($CaTiSiO_5$). J Am Ceram Soc 76: 4320–4321

Kunz M, Xirouchakis D, Lindsley DH, Hauserman D (1996) High-pressure transition in titanite ($CaTiOSiO_4$). Am Mineral 81: 1527–1530

LeBail A (1992) Extracting structure factors from powder diffraction data by iterating full pattern profile fitting. In: Prince E, Scalick JK (eds) Accuracy in powder diffraction II, Special Publication 846, 213 p. National Institute of Standards and Technology, Gaithersburg, Md

Manning CE, Bohlen SR (1991) The reaction titanite + kyanite = anorthite + rutile and titanite-rutile barometry in eclogites. Contrib Mineral Petrol 109: 1–9

Mraw SC (1988) Differential scanning calorimetry. In: Ho CY (ed) Specific Heat of Solids, CINDAS Data Series on Material Properties. Vol I-2. Hemisphere Publishing Corporation, New York, pp 395–437

Prince AT (1945) The system albite-anorthite-sphene. J Geol 51: 1–16

Richet P, Bottinga Y (1982) Modèles de calcul des capacités calorifiques des liquides et des verres silicatés. CR Acad Sci Paris 295: 1121–1124

Richet P (1987) Heat capacity of silicate glasses. Chem Geol 62: 111–124

Robie RA, Hemingway BS, Fisher JR (1978) Thermodynamic properties of minerals and related substances at 298.15 and 1 bar (10^5 pascals) pressure and higher temperatures. Geol Surv Bull 1452

Robie RA, Hemingway BS (1995) Thermodynamic properties of minerals and related substances at 298.15 K and 1 Bar (10^5 Pascals) Pressure and Higher Temperatures. Geol Soc Bull 2131

Robbins CR (1968) Synthetic $CaTiSiO_5$ and its germanium analogue ($CaTiGeO_5$). Mater Res Bull 3: 693–698

Tanaka I, Obuchi T, Kojima H (1988) Growth and characterization of titanite ($CaTiSiO_5$) single crystals by the floating zone method. J Crystallogr Growth 87: 169–174

Tangeman JA (1998) Thermodynamic and transport properties of iron-bearing silicate melts. PhD thesis, University of Michigan

Tangeman JA, Lange RA (1998) The effect of Al^{3+}, Fe^{3+}, and Ti^{4+} on the configurational heat capacities of sodium silicate liquids. Phys Chem Miner 26: 83–99

Thiéblot L, Téqui C, Richet P (1999) High-temperature heat capacity of grossular ($Ca_3Al_2Si_3O_{12}$), enstatite ($MgSiO_3$), and titanite ($CaTiSiO_5$). Am Mineral 84: 948–855

Taylor M, Brown GE (1976) High-temperature structural study of the $P2_1/a \leftrightarrow A2/a$ phase transition in synthetic titanite, $CaTiSiO_5$. Am Mineral 61: 435–447

Todd SS, Kelley KK (1956) Heat and free-energy data for tricalcium dititanate, sphene, lithium metatitanate, and zinc-titanium spinel. US Bureau of Mines Report of Investigations 5193

Wones DR (1989) Significance of the assemblage titanite + magnetite + quartz in granitic rocks. Am Mineral 74: 744–749

Xirouchakis D, Lindsley DH (2000) Interpreting assemblages with titanite (sphene): it does not have to be Greek to you. American Geophysical Union, Spring meeting. Special session on accessory minerals

Xirouchakis D, Lindsley DH (1998a) Equilibria among titanite, hedenbergite, fayalite, ilmenite, and magnetite: experiments and internally consistent thermodynamic data for titanite. Am Mineral 83: 712–725

Xirouchakis D, Lindsley DH (1998b) Oxide-silicate equilibria: assemblages with titanite. Experimental mineralogy, petrology, and geochemistry VII, TERRA Abstracts, suppl. 1, 10: 69–70

Xirouchakis D, Kunz M, Parise JB, Lindsley DH (1997a) Synthesis methods and unit cell volume of end-member titanite ($CaTiOSiO_4$). Am Mineral 82: 748–753

Xirouchakis D, Fritsch S, Putnam RL, Navrotsky A, Lindsley DH (1997b) Thermochemistry and enthalpy of formation of synthetic end-member ($CaTiSiO_5$) titanite. Am Mineral 82: 754–759

Xirouchakis D, Lindsley DH (1995) Low-pressure equilibria among titanite (sphene), hedenbergite, iron titanium oxides, and silica: experiments and internally consistent thermodynamic data for titanite. VM Goldschmidt Conference, Programs with Abstracts p 98. PENNSTATE

Zachariassen WH (1930) The crystal structure of titanite. Z Kristallogr 73: 7–16

Zhang M, Salje EKH, Bismayer U, Unruh HG, Wruck B, Schmidt C (1995) Phase transition(s) in titanite $CaTiSiO_5$. Phys Chem Mineral 22: 41–49

Zhang M, Salje EKH, Bismayer U (1997) Structural phase transition near 825 K in titanite: evidence from infrared spectroscopic observation. Am Mineral 82: 30–35